

# Simultaneously exploring multi-scale and asymmetric EEG features for emotion recognition

Yihan Wu<sup>a</sup>, Min Xia<sup>a</sup>, Li Nie<sup>a</sup>, Yangsong Zhang<sup>a,b,\*</sup>, Andong Fan<sup>c,\*</sup>

<sup>a</sup>*School of Computer Science and Technology, Southwest University of Science and Technology, Mianyang 621010, China*

<sup>b</sup>*Key Laboratory of Cognition and Personality, Ministry of Education, Chongqing, China*

<sup>c</sup>*College of Mathematics and Physics, Chengdu University of Technology, Chengdu 610059, China*

---

## Abstract

In recent years, emotion recognition based on electroencephalography (EEG) has received growing interest in the brain-computer interaction (BCI) field. The neuroscience researches indicate that the left and right brain hemispheres demonstrate differences under different emotional activities, which could be an important principle for designing deep learning (DL) model for emotion recognition. Besides, owing to the nonstationarity of EEG signals, using convolution kernel with a single size may not sufficiently extract the useful features. Based on these two angles, we proposed a model termed Multi-Scales Bi-hemispheric Asymmetric Model (MSBAM) based on convolutional neural network (CNN) structure. Evaluated on the public DEAP dataset, the MSBAM achieved over 96% accuracy of binary classification task in the four dimensions, i.e, arousal, valence, dominance and liking. This study further demonstrated the promising potential to design the DL model from the multi-scale characteristics of the EEG data and the neural mechanisms from the emotion cognition.

## Keywords:

Emotion recognition, EEG, Deep learning, Convolutional neural networks

---



---

\*Corresponding Authors: zhangysacademy@gmail.com; fad@cdut.edu.cn

## 1. Introduction

Emotion is a kind of physiological and psychological phenomenon playing a significant role in daily life[1][2]. In recent years, emotion recognition based on machine learning and deep learning(DL) methods has attracted growing attention of the research community [3]. Emotions can be detected from different modalities, such as facial expression [4], speech [5], and physiological data [6], etc. Among these, the physiological signals are hard to fake and show a decided advantage in measurement of spontaneous mental activity under different emotion states.

Human physiological signals can be measured by different imaging modalities, such as functional magnetic resonance imaging (fMRI), magnetoencephalography (MEG), functional near-infrared spectroscopy (fNIRS), and electroencephalography (EEG), et al. Benefiting from the properties such as high temporal resolution, non-invasive, low cost, and the portability of devices, EEG has been widely employed in the emotion recognition field [7].

To differentiate emotional states, the conventional approaches adopt feature extractor plus classifier to build the algorithms. Various hand-crafted features have been employed to extract the differences between different emotional states. For instance, Wen et al. utilized Pearson correlation coefficient (PCC) to estimate the correlation between all channel pairs, and achieved 77.98% and 72.98% average accuracy in valance and arousal of the DEAP dataset, respectively [8]. Zheng et al. extracted power spectral density (PSD), differential entropy (DE), differential asymmetry, rational asymmetry, asymmetry and differential causality features in their study [9]. Their classifier obtained 69.67% accuracy for four classification task on valance-arousal space. Moon et al. employed PCC, phase-locking value (PLV) and transfer entropy (TE) to conduct their experiment [10]. They utilized samples of 3 second length to train their model and achieved 87.75% accuracy in valance dimension.

With the rapid development of DL, increasing researchers pursue end-to-end solutions to replace the conventional classification methods based on handcraft features. Yang et al. proposed parallel convolutional recurrent neural network combining convolutional neural networks(CNN) and Long-Short Term Memories neural network(LSTM) [11]. Their method achieved 90.80% and 91.03% performance on valance and arousal of DEAP with 1 second samples, respectively. Ma et al. proposed a method, which applied residual structure on LSTM [12]. This method obtained 92.30% and 92.87%

accuracy on valence and arousal of DEAP dataset with 1 second EEG data, respectively. Yin et al. proposed a method fusing graph convolutional neural networks and LSTM and obtained 90.45% and 90.60% accuracy on DEAP with 6 second samples, respectively. [13]

For the past few years, increasing studies have started to design the DL models by considering the physiological mechanisms of emotions. Bi-hemispheric discrepancy under different emotion states is a vital neural mechanism, which has been used in several studies with DL models for emotion recognition [14, 15]. For instance, Li et al. proposed a method using LSTM to capture the features of bi-hemispheric discrepancy [14]. Their model yielded 92.38% and 84.14% accuracy on the subject dependent and independent task on the SEED dataset, respectively. In another study, Li et al. proposed a method termed R2G-STNN [16]. They extracted regional features according to the spatial region concerning physiological function, and fused the regional and global features. This method achieved 93.38% and 84.16% accuracy on the SEED dataset [16].

EEG signals are nonstationary, using a single convolution kernel size may not sufficiently extract the useful features. Previous studies have demonstrated that using multiple convolution kernels of different size could learn multi-scale EEG features which is beneficial for different EEG classification tasks [17]. For example, Li et al. proposed a multi-scale fusion CNN model for motor imagery classification [18]. The experimental results indicated that the model achieved a better performance compared with the baseline methods. The multi-scale CNN has also been introduced in emotion recognition. Phan et al. proposed a 2D CNN model with multi-scale kernels for arousal and valence binary classification [19].

However, the physiological mechanisms and multi-scale features of EEG has not been simultaneously considered in a DL model for emotion recognition. Based on this consideration, we proposed a DL model termed Multi-Scales Bi-hemispheric Asymmetric Model (MSBAM) to explore the multi-scale asymmetric information. MSBAM is composed of the parallel spatial-domain feature extractor and multi-scales temporal-domain feature extractor, followed by a fully connected layer classifier. We conducted extensive experiments on the public DEAP dataset. The results indicate that our MSBAM achieve better performance than the baseline methods.

The remainder of this paper is organized as follows. Section 2 introduces materials and methods. Section 3 describes the settings and results of extensive experiments, comparisons between MSBAM and the baseline methods

are also be provided in this section. Section 4 and 5 present the discussions and conclusion.

## 2. Materials and Methods

### 2.1. DEAP dataset

The public DEAP dataset was adopted to validate the performance of our MSBAM, which is the most widely used in emotion recognition domain. The DEAP dataset is a multimodal dataset first presented by Koelstra and colleagues[20]. Thirty-two healthy subjects participated in the experiment. They were watching 40 one-minute pieces of music videos. The EEG and peripheral physiological signals were recorded when they were watching videos. Forty electrodes (32 for EEG and 8 for peripheral physiological signals) were applied in the recording. Participants were asked to rate each video from 1 to 9 to evaluate the levels of four dimensions, i.e., arousal, valence, dominance and liking, respectively. Each trial contains 3 s baseline data and 60 s task data. For the offline analysis, the EEG signals were first downsampled to 128 Hz from 512 Hz, and referred to the common reference. Electrooculogram (EOG) artifacts were removed. Then, the EEG data was filtered by a bandpass filter with 4-45 Hz. The details can be found in the reference [20].

The class labels in the DEAP dataset for each dimension range from 1 to 9. For the binary classification, the labels of the data in the four dimensions (arousal, valence, dominance and liking) are respectively set to low and high by the threshold of score 5 as the previous studies [21, 22].

### 2.2. Data processing

In order to reduce the noise and improve the stability of the signal, baseline correction and z-score normalization were implemented on the dataset, which were commonly pre-processing procedures for EEG [15, 23]. Previous studies demonstrated that these operations can improve emotion recognition accuracy by reducing the interference of basic emotional state before the task period [24]. The diagram of baseline correction is illustrated in the Fig. 1.

First, the 3 s baseline data were divided into three segments of 1 s length without overlap. These segments were further averaged to obtain the baseline signal of 1 s length, called resting-state segment. Second, the 60 s task data of each trial were divided into 60 segments of 1 s length without overlap, termed task-state segments. Third, each task-state segment subtracted the resting-state segment. After these steps, we concatenated all the processed

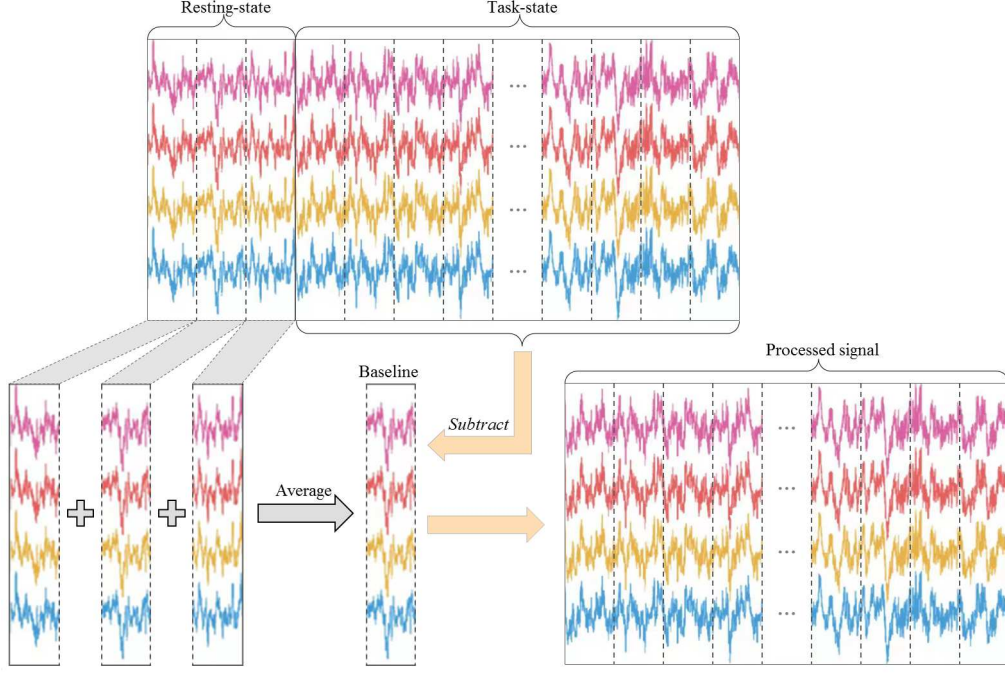


Figure 1: The diagram of baseline correction for the DEAP dataset. The first 3 seconds is regarded as resting-state data. All the task-state data should subtract the average signal of resting-state second by second.

task-state segments to construct the new task-state data of 60 s. At the last, z-score normalization was utilized on each channel of the task-state data.

After the pre-processing procedure, the new task-state data will be segmented with  $Wnd$  seconds window without overlap. Finally, we obtained samples  $D \in \mathbb{R}^{C \times T}$ , where  $C$  denotes the number of channels and  $T = Fs * Wnd$  represents the number of sample points.  $Fs$  denotes the sampling rate of 128 Hz. For the parameter  $Wnd$ , we set it to be 1 in the following experiments as that in the previous studies [15, 25, 22].

### 2.3. 3D representation of the EEG data

Traditionally, EEG data is represented as 2D matrix with the shape of channels  $\times$  sample points for most algorithms. Under the 2D representation, the data from all used channels at a sampling time point are arranged into a column vector, the topological information among different channels would be lost. In recent years, the 3D representation has been introduced for EEG

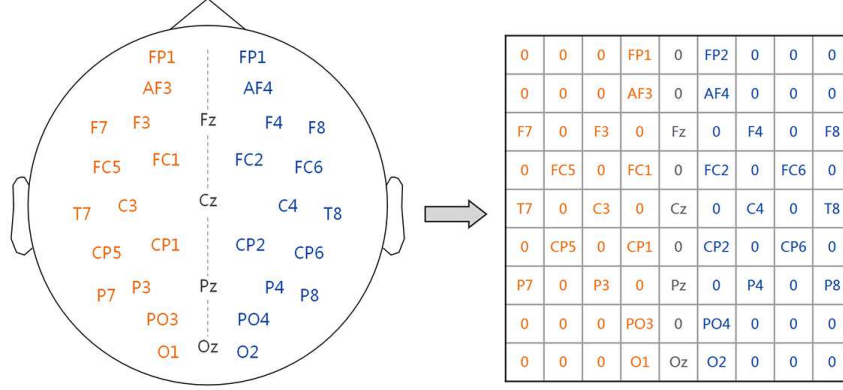


Figure 2: A schematic diagram of a 2D representation of EEG channel locations with a  $9 \times 9$  matrix at each sample point.

data [26]. In this way, the data from all used channels at one sample point are arranged into a 2D matrix according to distribution of the international 10-20 system, which can retain the spatial information among channels to some extent. We denote this operation as spatial transformation. The schematic diagram is shown in Fig. 2. We implement the spatial transformation at all sample points to obtain the 3D representation of the EEG data. This 3D representation can preserve both temporal information and spatial information of EEG data, which has been adopted for various EEG classification tasks [23, 27, 28].

As the input of our model, each sample  $D \in \mathbb{R}^{C \times T}$  is transformed to a 3D spatial-temporal matrix  $D \in \mathbb{R}^{H \times W \times T}$ . In current study,  $C = 32$ ,  $T = 128$ , and  $H$  and  $W$  are set to 9.

#### 2.4. The construction of proposed MSBAM

Previous studies indicate the significance of physiological mechanisms and multi-scale features of EEG for emotion recognition [14, 19]. However, the correlations and differences of asymmetric features in various time scales have not been considered in a DL model for emotion recognition. Based on this consideration, our MSBAM contains three parts, i.e., a spatial feature extractor block, a temporal feature extractor block, and a feature classification block. The structure and details of MSBAM are shown in Figs. 3, 4 and 5, respectively.

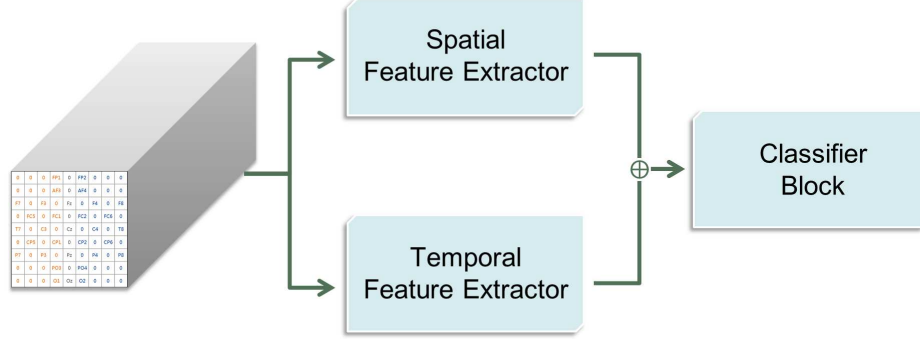


Figure 3: The structure of MSBAM.

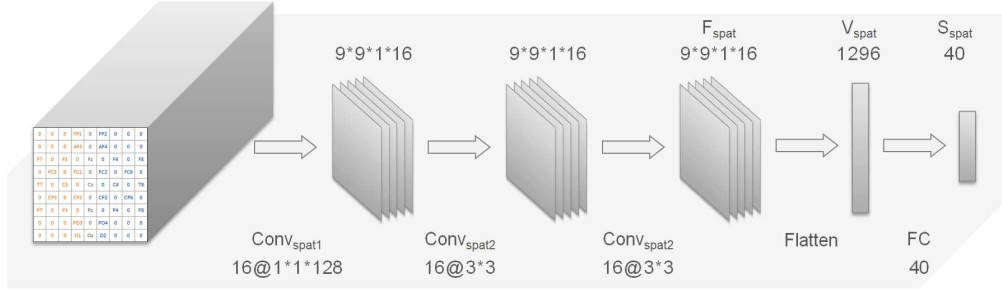


Figure 4: A schematic diagram of overall structure of the spatial feature extractor block.

#### 2.4.1. Spatial feature extractor block

For the spatial feature extractor block, as shown in Fig. 4, it contains three convolution blocks (Conv) and one fully connected block (FC). The first Conv block, denoted as  $Conv_{spat1}$ , contains a convolution operator( $conv_1$ ) with 16 kernels of size  $1 \times 1 \times 128$ , and a Scaled Exponential Linear Units (SELU) activation function, which is expressed as:

$$Conv_{spat1}(\cdot) = \sigma(conv_1(\cdot)) \quad (1)$$

where  $\sigma$  denotes the SELU function. This procedure is able to compress the data from 3 D into 2 D, and all values in the time dimension are transformed to single feature value. The remaining two Conv blocks are similar to the  $Conv_{spat1}$  except for the convolution operator, where 32 kernels of size  $3 \times 3$  and padding size of (1, 1) are used to extract high-level spatial information. Through these Conv blocks successively, a feature  $F_{spat} \in \mathbb{R}^{9 \times 9 \times 1 \times 16}$  is

obtained to represent the spatial feature of the EEG data.

Then the feature  $F_{spat}$  is flattened to a vector and input into a FC layer followed by a batch normalization layer and softmax activation to obtain the normalized feature  $S_{spat}$ , which could be described as:

$$V_{spat} = Flatten(F_{spat}) \quad (2)$$

$$V_{fc} = BN(W \cdot V_{spat} + b) = [V_1, V_2, \dots, V_{40}] \in \mathbb{R}^{40} \quad (3)$$

$$\bar{V}_i = \frac{\exp(V_i)}{\sum_{k=1}^{40} \exp(V_k)}, i = 1, 2, \dots, 40 \quad (4)$$

$$S_{spat} = [\bar{V}_1, \bar{V}_2, \dots, \bar{V}_{40}] \in \mathbb{R}^{40} \quad (5)$$

where  $W$  is the weight matrix,  $b$  is the bias. The procedure of formulas (3) (4) and (5) are denoted as the *FeatureNormalizationLayer*, and will be utilized in the temporal feature extractor block.

#### 2.4.2. Temporal feature extractor block

For the temporal feature extractor block, as is shown in Fig. 5(a), it contains  $K$  branches, each of which contains a convolution block named  $Conv_{temp}^k$ , a flatten-concatenation operation, and a *FeatureNormalizationLayer*. Multiple branches by using several temporal convolution kernels of different length could learn multi-scale EEG features which is beneficial for emotion recognition task.

In each branch, the EEG data  $D$  is split into two parts in spatial dimension. As shown in Fig. 5(b), The first part, denoted as  $D_l \in \mathbb{R}^{9 \times 5 \times 128}$ , comes from the columns of [1, 2, 3, 4, 5] of the  $9 \times 9$  matrix as shown in Fig. 2, which represents the data from left hemisphere. Similarly, the second part, denoted as  $D_r \in \mathbb{R}^{9 \times 5 \times 128}$ , comes from the columns of [5, 6, 7, 8, 9], which represents the data from right hemisphere. To remain the unified location of electrodes between  $D_l$  and  $D_r$ , a horizontal flip is implemented on  $D_r$ , which rearranges the columns as [9, 8, 7, 6, 5]. After the process,  $D_l$  and  $D_r$  are first input into the same  $Conv_{temp}^k$  block, which is illustrated in the following:

$$Conv_{temp}^k(\cdot) = \sigma(conv_k(\cdot)) \quad (6)$$

where  $k$  denotes  $k$ -th branch, and  $\sigma$  is SELU activation function. The  $conv_k$  conducts a 3D convolution with 16 kernels of size  $9 \times 5 \times L_i$  and the stride of size  $9 \times 5 \times S_i$ . The  $L_i$  is the time scale of the extractor, and the  $S_i$  is equal to  $L_i/2$ .



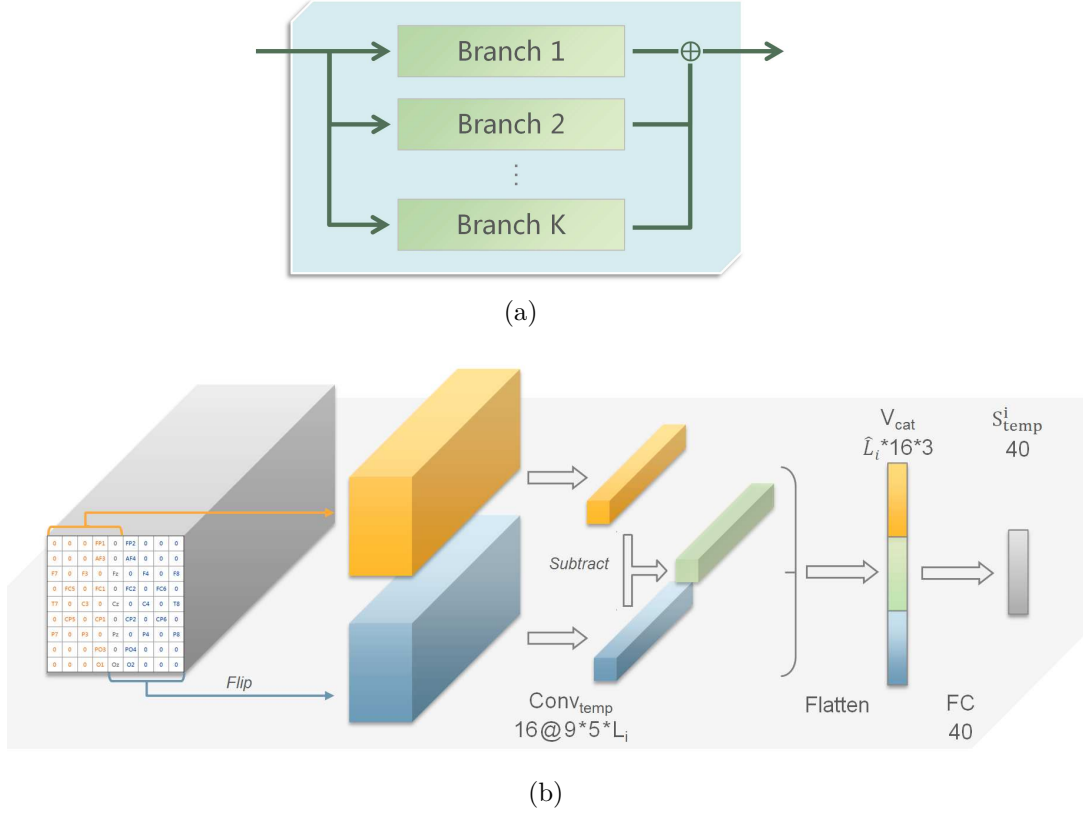


Figure 5: (a) shows overall structure of the temporal feature extractor block.  $K$  denotes the number of branches, and  $K=3$  is a proper configuration proved by our experiment. (b) shows the  $i$ -th bi-hemispheric asymmetric feature extractor.

After the  $Conv_{temp}$  block, the  $F_l$  and  $F_r$  are obtained and utilized to calculate discrepant feature, which is denoted as  $F_a \in \mathbb{R}^{1 \times 1 \times \hat{L} \times 16}$ . The calculation is described as follows:

$$F_a = F_l - F_r \quad (7)$$

After that, these three kinds of features, i.e.,  $F_l$ ,  $F_r$  and  $F_a$ , are first flattened to vectors ( $V_l \in \mathbb{R}^{\hat{L} \times 16}$ ,  $V_r \in \mathbb{R}^{\hat{L} \times 16}$ , and  $V_a \in \mathbb{R}^{\hat{L} \times 16}$ ), further combined into a vector  $V_{cat} \in \mathbb{R}^{\hat{L} \times 16 \times 3}$ . Then, the feature  $V_{cat}$  is input into *FeatureNormalizationLayer* to achieve unified representation. We denoted the  $i$ -th feature from  $i$ -th branch as  $S_{temp}^i \in \mathbb{R}^{40}$ .

Finally, all the  $K$  features from all the  $K$  branches were concatenated as

one vector  $S_{temp}$ :

$$S_{temp} = [S_{temp}^1 \parallel S_{temp}^2 \parallel \dots \parallel S_{temp}^K] \in \mathbb{R}^{40 \times K} \quad (8)$$

After these procedures above, we obtain the asymmetric features on multiple time scales. Those features would be input into the feature concatenation and classification block along with  $S_{spat}$ .

#### 2.4.3. Feature classification block

Through the previous procedures, we obtain two groups of features, i.e.,  $S_{spat}$  and  $S_{temp}$ . These features are first concatenated to a integrated vector  $S_{cat}$ , which is called final feature map. The final feature map will be used to visualize the model in the following analysis. Through a dropout with the rate of 0.7, the feature is input into a FC layer with two neurons. The output feature is regarded as the possibility( $P(c|D)$ ,  $c = 0, 1$ ) that the EEG data  $D$  belongs to each class. The predicted label is that of the class which has maximal possibility. The procedure could be described as:

$$y_{pred} = \arg \max_c P(c|D), c = 0, 1. \quad (9)$$

where the  $P(c|D)$  is the possibility of  $D$  belonging to the  $c$ -th class.

#### 2.5. Baseline methods

To verify the performance of our model, we compared the MSBAM with ten baseline methods, which were evaluated on the DEAP dataset. These methods are introduced briefly as follows:

**The method of Liu-2019.** Liu et al. introduced a method named deep canonical correlation analysis(DCCA) [29]. The raw EEG signals and peripheral physiological features was transformed by different nonlinear networks to obtain the two groups of features. Those features were fused by a weighted sum method after being regularized with the traditional CCA method. Then, the fusion features were used to train a linear SVM classifier for emotion recognition.

**The method of Qiu-2018.** Qiu et al. proposed a multimodal emotion recognition method named correlated attention network (CAN) [30]. They extracted features with two Bidirectional Gated Recurrent Unit (GRU) neural networks, and applied a canonical correlation to calculate the correlation. In the end, attention mechanism was utilized to implement the emotion classification task.

**The method of Yin-2021.** Yin et al. proposed a ECLGCNN model which fused LSTM and GCNN for emotion classification [31]. In the GCNN model, the EEG channels and functional connections between two channels were denoted as the vertex nodes and edges, respectively. The greater value of the edge means the closer relationship between two channels. The features extracted by the GCNNs were input into LSTM networks to extract the higher level features for emotion classification tasks.

**The method of Yang-2018.** Yang et al. introduced a pre-processing method for baseline correction, and validated it with their new model termed as parallel convolutional recurrent neural network (PCRNN) [11]. In this model, the pre-processed 2D EEG signals were transformed into 3D representation according to the spatial topology of electrodes. Then a group of CNNs and LSTMs were utilized to extract the spatial and temporal features, respectively. To classify the emotion states, these features were concatenated and input into a fully connected layer.

**The method of Liao-2020.** Liao et al. proposed a multimodal emotion recognition method [32]. They transformed the raw EEG signal into 3D representation as in the studied by Yang et al [11]. 2D-CNNs were employed to extract the spatial features of EEG signals, and LSTM were utilized to extract the temporal features of peripheral physiological signals. The concatenated spatial and temporal features were fed into a softmax classifier to predict the emotion states.

**The method of Ma-2019.** Ma et al. proposed a method named MM-ResLSTM based on EEG and peripheral physiological signals [25]. MM-ResLSTM contains four LSTMs, and the last three of them have a residual structure. Multimodal data were fed into two MMResLSTM modules that shared parameters to extract the high-level features, and then concatenated to predict the emotion state by a softmax layer.

**The method of Huang-2021.** Huang et al. released a method based on the discrepancy of emotional response between two hemispheres, which was named bi-hemisphere discrepancy convolutional neural network (BiDCNN) [15]. Three different matrices were constructed and input into the BiDCNN to extract the spatial and temporal features, including the discrepancy features of emotional responses between left and right hemispheres. In the end, all the features were concatenated and fed into a series of convolution layers and dense layers to predict the emotion state.

**The method of Li-2021.** Li et al. proposed a method named dilated fully convolutional networks (DFCN) [22]. They filtered the raw data into

four frequency bands, and calculated three kind of features, i.e., Kurtosis feature, Power feature, and DE feature, in each frequency band. Those features were rearranged to a 3D representation. The DFCN contains two convolution layers, three dilated convolution layers and two linear layers. They introduced Spectral Norm Regularization (SNR) to reduce the sensitivity of distribution.

### 2.6. Model implementation

For the MSBAM, the cross-entropy was employed as the loss function. Adam optimizer was utilized to minimize the loss function with 0.001 learning rate initially. The experiment performed 150 epochs, and the learning rate was reduced to 0.0001 at the 120th epoch. For utilizing the experiment, the number of branches in the proposed MSBAM model was set to 3, and the parameters of time scales ( $L_i$ ) in the three branches in temporal feature extractor were set to 128, 96, 64, respectively.

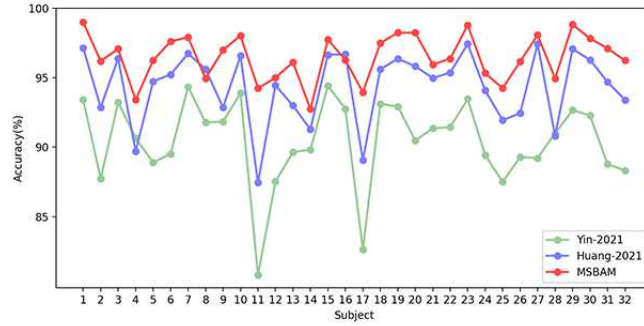
For each subject, the 10-fold cross validation was used for emotion recognition. Average accuracy was used to evaluate the performance of MSBAM and baseline models.

## 3. Results

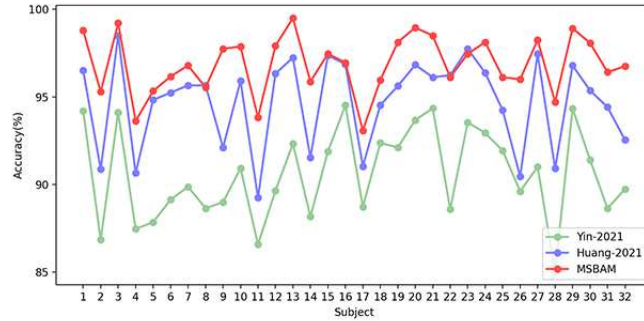
Table 1: Accuracies of the MSBAM and other baseline methods (mean  $\pm$  std.). The symbol “/” indicates values of methods are not provided in original studies.

Methods	Valence(%)	Arousal(%)	Dominance(%)	Liking(%)
Tang-2017[33]	83.82 $\pm$ 5.01	83.23 $\pm$ 2.61	/	/
Liu-2016[21]	85.20 $\pm$ /	80.50 $\pm$ /	84.90 $\pm$ /	82.40 $\pm$ /
Liu-2019[29]	85.62 $\pm$ 3.48	84.33 $\pm$ 2.25	90.67 $\pm$ 4.33	/
Qiu-2018[30]	86.45 $\pm$ /	84.79 $\pm$ /	/	/
Yin-2021[31]	90.45 $\pm$ 3.09	90.60 $\pm$ 2.62	/	/
Yang-2018[34]	90.80 $\pm$ 3.08	91.03 $\pm$ 2.99	/	/
Liao-2020[32]	91.95 $\pm$ /	93.06 $\pm$ /	/	/
Ma-2019[25]	92.30 $\pm$ 1.55	92.87 $\pm$ 2.11	/	/
Huang-2021[15]	94.38 $\pm$ 2.61	94.72 $\pm$ 2.56	/	/
Li-2021[22]	94.59 $\pm$ /	95.32 $\pm$ /	94.78 $\pm$ /	95.19 $\pm$ /
<b>MSBAM</b>	<b>96.48 <math>\pm</math> 1.59</b>	<b>96.86 <math>\pm</math> 1.76</b>	<b>97.02 <math>\pm</math> 1.76</b>	<b>97.09 <math>\pm</math> 1.84</b>

We respectively conducted the experiments in *valence*, *arousal*, *dominance* and *liking* dimensions to verify the effectiveness of the MSBAM, and compare its performance with the baseline methods. The experimental results of all methods are summarized in Table 1. We could find that our MSBAM yields better performance than the baseline methods. Compared with the best baseline model, MSBAM could improve average recognition accuracy by 1.89%, 1.54%, 2.24% and 1.90% in *valence*, *arousal*, *dominance* and *liking* dimensions, respectively. In addition, MSBAM achieves smaller standard deviation than the best baseline method. It indicates that MSBAM has better robustness than the baseline methods.



(a)



(b)

Figure 6: Average for every subject on *Valance*(a) and *Arousal*(b) dimension.

To observe the performance of proposed MSBAM of each subject, two line charts are presented in Fig. 6(a) and Fig. 6(b). In the chart, we only present

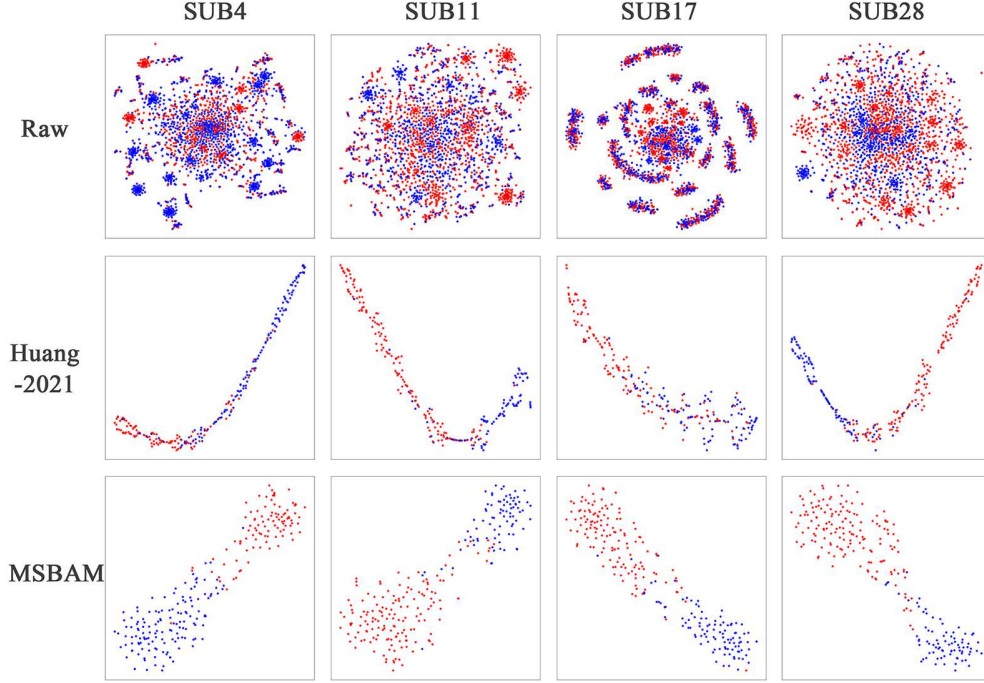


Figure 7: Visualization of the final feature maps using t-SNE. The final feature maps are features before the last FC layer(e.g. the  $S_{cat}$  in the proposed MSBAM).

the results from two baseline methods, i.e., *Yin – 2021* and *Huang – 2021*, which provided the accuracy information for each subject in the original paper. We could find that all the methods yield analogical tendencies as the subject changes. The MSBAM shows better performance than other models. It has the best accuracy on the most subjects.

To further investigate the results of MSBAM, the features before the last FC layer(final feature map) in *Valence* dimension were visualized by the t-SNE[35]. Four subjects with lowest accuracies were selected. The features of t-SNE are shown in Fig. 7. The first row in the figure illustrated all the original data. The second and the last row presented the test set in the first fold of each subject. Because of lacking related information in the paper[15], we re-produced the method using the similar hyper-parameter with our MSBAM. We could observe that the proposed MSBAM have better intra-category similarity and inter-category separability than the baseline method.

#### 4. Discussions

The experimental results demonstrate that the proposed MSBAM model outperforms other baseline methods. This may be attributed to the model structure that extracts the features of multi-scale and bi-hemispheric asymmetry, simultaneously. To further verify the rationality of the MSBAM, several ablation experiments were conducted. First, we need to check that the spatial feature extractor and three branches in temporal feature extractor block are appropriate. The results of several ablation experiments are shown in Table 2. MSBAM- $r_i$  means that the  $i$ -th branch in the temporal feature extractor block is removed, and the MSBAM-rSpat means the spatial feature extractor is dropped, in the original MSBAM. We could find that removing parts of the branches in temporal feature extractor block, or the spatial feature extractor will reduce the accuracies obtained by the original MSBAM.

Table 2: Average accuracy(%) of the multi-scales ablation experiments(mean  $\pm$  std.).

Methods	Valence(%)	Arousal(%)	Dominance(%)	Liking(%)
MSBAM-r2-r3	95.70 $\pm$ 1.88	96.09 $\pm$ 2.00	96.36 $\pm$ 2.00	96.34 $\pm$ 2.28
MSBAM-r1-r3	95.68 $\pm$ 1.89	96.15 $\pm$ 1.95	96.40 $\pm$ 1.98	96.26 $\pm$ 2.39
MSBAM-r1-r2	95.81 $\pm$ 1.84	96.27 $\pm$ 1.91	96.50 $\pm$ 1.90	96.45 $\pm$ 2.23
MSBAM-r1	96.19 $\pm$ 1.67	96.77 $\pm$ 1.73	96.90 $\pm$ 1.74	96.92 $\pm$ 2.13
MSBAM-r2	96.27 $\pm$ 1.66	96.67 $\pm$ 1.88	96.90 $\pm$ 1.76	96.83 $\pm$ 2.10
MSBAM-r3	96.30 $\pm$ 1.64	96.64 $\pm$ 1.80	96.85 $\pm$ 1.79	96.79 $\pm$ 2.06
MSBAM-rSpat	96.29 $\pm$ 1.73	96.71 $\pm$ 1.84	96.87 $\pm$ 1.80	96.85 $\pm$ 2.08
<b>MSBAM</b>	<b>96.48 <math>\pm</math> 1.59</b>	<b>96.86 <math>\pm</math> 1.76</b>	<b>97.02 <math>\pm</math> 1.76</b>	<b>97.09 <math>\pm</math> 1.84</b>

Although the MSBAM shows better performance than all the baseline methods, some limitations should be mentioned. In current study, only the DEAP dataset was adopted to evaluate the performance, more datasets should be used to verify the effectiveness of the proposed MSBAM. Besides, in the Table 1, we could find that all methods can obtain accuracy above 80%. However, there exists a problem of data leakage because of the approach to obtain the training data and testing data for all the trial-dependent method, which is a common phenomenon in existing DL models [36, 37]. A few studies try to evaluate the DL models on more challenging scenarios, trial-independent classification within subject [36, 37] and subject-independent

classification [38, 39]. Those two scenarios should be adopted in future studies when we evaluate the DL models to avoid data leakage and biased evaluation.

## 5. Conclusion

In this paper, we propose an emotion recognition method based on multi-scale and bi-hemispheric asymmetric features, termed MSBAM. The proposed MSBAM could achieve average accuracies of 96.48%, 96.86%, 97.02% and 97.09% in *Valence*, *Arousal*, *Dominance* and *Liking* dimensions respectively, which outperformed all the baseline methods in the subject-dependent classification scenario. Although some limitations should be addressed in future studies, current study demonstrates that exploring the multi-scale features and utilizing the neural mechanism of the emotions such as the bi-hemispheric asymmetry to design the DL model, are beneficial for emotion recognition.

## Acknowledgments

This work was supported in part by the National Natural Science Foundation of China under Grant No.62076209.

## References

- [1] R. J. Dolan, Emotion, cognition, and behavior, *Science* 298 (5596) (2002) 1191–1194.
- [2] M. Cabanac, What is emotion?, *Behavioural Processes* 60 (2) (2002) 69–83.
- [3] E. P. Torres, E. A. Torres, M. Hernández-Álvarez, S. G. Yoo, EEG-based BCI emotion recognition: a survey, *Sensors* 20 (18) (2020) 5083.
- [4] S. Zhao, H. Tao, Y. Zhang, T. Xu, K. Zhang, Z. Hao, E. Chen, A two-stage 3d CNN based learning method for spontaneous micro-expression recognition, *Neurocomputing* 448 (2021) 276–289.
- [5] M. El Ayadi, M. S. Kamel, F. Karray, Survey on speech emotion recognition: Features, classification schemes, and databases, *Pattern Recognition* 44 (3) (2011) 572–587.



- [6] P. Li, H. Liu, Y. Si, C. Li, F. Li, X. Zhu, X. Huang, Y. Zeng, D. Yao, Y. Zhang, P. Xu, EEG based emotion recognition by combining functional connectivity network and local activations, *IEEE Transactions on Biomedical Engineering* 66 (10) (2019) 2869–2881. doi:10.1109/TBME.2019.2897651.
- [7] W. Li, W. Huan, B. Hou, Y. Tian, Z. Zhang, A. Song, Can emotion be transferred? – a review on transfer learning for EEG-based emotion recognition, *IEEE Transactions on Cognitive and Developmental Systems* (2021) 1–1doi:10.1109/TCDS.2021.3098842.
- [8] Z. Wen, R. Xu, J. Du, A novel convolutional neural networks for emotion recognition based on EEG signal, in: 2017 International Conference on Security, Pattern Analysis, and Cybernetics (SPAC), 2017, pp. 672–677. doi:10.1109/SPAC.2017.8304360.
- [9] W.-L. Zheng, J.-Y. Zhu, B.-L. Lu, Identifying stable patterns over time for emotion recognition from EEG, *IEEE Transactions on Affective Computing* 10 (3) (2019) 417–429. doi:10.1109/TAFFC.2017.2712143.
- [10] S.-E. Moon, C.-J. Chen, C.-J. Hsieh, J.-L. Wang, J.-S. Lee, Emotional eeg classification using connectivity features and convolutional neural networks, *Neural Networks* 132 (2020) 96–107.
- [11] Y. Yang, Q. Wu, M. Qiu, Y. Wang, X. Chen, Emotion recognition from multi-channel EEG through parallel convolutional recurrent neural network, in: 2018 International Joint Conference on Neural Networks (IJCNN), 2018, pp. 1–7. doi:10.1109/IJCNN.2018.8489331.
- [12] J. Ma, H. Tang, W.-L. Zheng, B.-L. Lu, Emotion recognition using multimodal residual LSTM network, in: Proceedings of the 27th ACM International Conference on Multimedia, MM '19, Association for Computing Machinery, New York, NY, USA, 2019, p. 176–183.
- [13] Y. Yin, X. Zheng, B. Hu, Y. Zhang, X. Cui, EEG emotion recognition using fusion model of graph convolutional neural networks and LSTM, *Applied Soft Computing* 100 (2021) 106954.
- [14] Y. Li, W. Zheng, Y. Zong, Z. Cui, T. Zhang, X. Zhou, A bi-hemisphere domain adversarial neural network model for EEG emotion recognition

- tion, *IEEE Transactions on Affective Computing* 12 (2) (2021) 494–504. doi:10.1109/TAFFC.2018.2885474.
- [15] D. Huang, S. Chen, C. Liu, L. Zheng, Z. Tian, D. Jiang, Differences first in asymmetric brain: A bi-hemisphere discrepancy convolutional neural network for EEG emotion recognition, *Neurocomputing* 448 (2021) 140–151.
  - [16] Y. Li, W. Zheng, L. Wang, Y. Zong, Z. Cui, From regional to global brain: A novel hierarchical spatial-temporal neural network model for EEG emotion recognition, *IEEE Transactions on Affective Computing* (2019) 1–1doi:10.1109/TAFFC.2019.2922912.
  - [17] W. Ko, E. Jeon, S. Jeong, H.-I. Suk, Multi-scale neural network for EEG representation learning in BCI, *IEEE Computational Intelligence Magazine* 16 (2) (2021) 31–45. doi:10.1109/MCI.2021.3061875.
  - [18] D. Li, J. Xu, J. Wang, X. Fang, Y. Ji, A multi-scale fusion convolutional neural network based on attention mechanism for the visualization analysis of EEG signals decoding, *IEEE Transactions on Neural Systems and Rehabilitation Engineering* 28 (12) (2020) 2615–2626. doi:10.1109/TNSRE.2020.3037326.
  - [19] T.-D.-T. Phan, S.-H. Kim, H.-J. Yang, G.-S. Lee, EEG-based emotion recognition by convolutional neural network with multi-scale kernels, *Sensors* 21 (15) (2021).
  - [20] S. Koelstra, C. Muhl, M. Soleymani, J.-S. Lee, A. Yazdani, T. Ebrahimi, T. Pun, A. Nijholt, I. Patras, DEAP: A database for emotion analysis ;using physiological signals, *IEEE Transactions on Affective Computing* 3 (1) (2012) 18–31.
  - [21] W. Liu, W.-L. Zheng, B.-L. Lu, Emotion recognition using multimodal deep learning, in: A. Hirose, S. Ozawa, K. Doya, K. Ikeda, M. Lee, D. Liu (Eds.), *Neural Information Processing*, Springer International Publishing, Cham, 2016, pp. 521–529.
  - [22] D. Li, B. Chai, Z. Wang, H. Yang, W. Du, EEG emotion recognition based on 3-D feature representation and dilated fully convolutional networks, *IEEE Transactions on Cognitive and Developmental Systems* 13 (4) (2021) 885–897. doi:10.1109/TCDS.2021.3051465.

- [23] H. Cui, A. Liu, X. Zhang, X. Chen, K. Wang, X. Chen, EEG-based emotion recognition using an end-to-end regional-asymmetric convolutional neural network, *Knowledge-Based Systems* 205 (2020) 106243.
- [24] Y. Yang, Q. Wu, M. Qiu, Y. Wang, X. Chen, Emotion recognition from multi-channel EEG through parallel convolutional recurrent neural network, in: *2018 International Joint Conference on Neural Networks (IJCNN)*, 2018, pp. 1–7. doi:10.1109/IJCNN.2018.8489331.
- [25] J. Ma, H. Tang, W.-L. Zheng, B.-L. Lu, Emotion recognition using multimodal residual LSTM network, in: *Proceedings of the 27th ACM International Conference on Multimedia, MM '19*, Association for Computing Machinery, New York, NY, USA, 2019, p. 176–183.
- [26] X. Zhao, H. Zhang, G. Zhu, F. You, S. Kuang, L. Sun, A multi-branch 3D convolutional neural network for EEG-based motor imagery classification, *IEEE Transactions on Neural Systems and Rehabilitation Engineering* 27 (10) (2019) 2164–2177.
- [27] Y. Zhang, H. Cai, L. Nie, P. Xu, S. Zhao, C. Guan, An end-to-end 3D convolutional neural network for decoding attentive mental state, *Neural Networks* 144 (2021) 129–137.
- [28] X. Zhao, H. Zhang, G. Zhu, F. You, S. Kuang, L. Sun, A multi-branch 3D convolutional neural network for EEG-based motor imagery classification, *IEEE Transactions on Neural Systems and Rehabilitation Engineering* 27 (10) (2019) 2164–2177. doi:10.1109/TNSRE.2019.2938295.
- [29] W. Liu, J.-L. Qiu, W.-L. Zheng, B.-L. Lu, Multimodal emotion recognition using deep canonical correlation analysis (2019). [arXiv:1908.05349](https://arxiv.org/abs/1908.05349).
- [30] J.-L. Qiu, X.-Y. Li, K. Hu, Correlated attention networks for multimodal emotion recognition, in: *2018 IEEE International Conference on Bioinformatics and Biomedicine (BIBM)*, 2018, pp. 2656–2660. doi:10.1109/BIBM.2018.8621129.
- [31] Y. Yin, X. Zheng, B. Hu, Y. Zhang, X. Cui, EEG emotion recognition using fusion model of graph convolutional neural networks and LSTM, *Applied Soft Computing* 100 (2021) 106954.

- [32] J. Liao, Q. Zhong, Y. Zhu, D. Cai, Multimodal physiological signal emotion recognition based on convolutional recurrent neural network, IOP Conference Series: Materials Science and Engineering 782 (2020) 032005. doi:10.1088/1757-899x/782/3/032005.
- [33] H. Tang, W. Liu, W.-L. Zheng, B.-L. Lu, Multimodal emotion recognition using deep neural networks, in: D. Liu, S. Xie, Y. Li, D. Zhao, E.-S. M. El-Alfy (Eds.), Neural Information Processing, Springer International Publishing, Cham, 2017, pp. 811–819.
- [34] Y. Yang, Q. Wu, M. Qiu, Y. Wang, X. Chen, Emotion recognition from multi-channel EEG through parallel convolutional recurrent neural network, in: 2018 International Joint Conference on Neural Networks (IJCNN), 2018, pp. 1–7. doi:10.1109/IJCNN.2018.8489331.
- [35] L. Van der Maaten, G. Hinton, Visualizing data using t-SNE., Journal of machine learning research 9 (11) (2008) 2579–2605.
- [36] Y. Ding, N. Robinson, Q. Zeng, C. Guan, TSception: Capturing temporal dynamics and spatial asymmetry from EEG for emotion recognition (2021). arXiv:2104.02935.
- [37] H. Wang, K. Liu, F. Qi, X. Deng, P. Li, EEG-based emotion recognition using convolutional neural network with functional connections, in: F. Sun, H. Liu, B. Fang (Eds.), Cognitive Systems and Signal Processing, Springer Singapore, Singapore, 2021, pp. 33–40.
- [38] J. Hu, C. Wang, Q. Jia, Q. Bu, R. Sutcliffe, J. Feng, ScalingNet: Extracting features from raw EEG data for emotion recognition, Neurocomputing 463 (2021) 177–184. doi:https://doi.org/10.1016/j.neucom.2021.08.018.
- [39] L.-M. Zhao, X. Yan, B.-L. Lu, Plug-and-play domain adaptation for cross-subject EEG-based emotion recognition, in: Proceedings of the 35th AAAI Conference on Artificial Intelligence, sn, 2021.